

---

## Gamma-Ray Detectors

---

*Hastings A. Smith, Jr., and Marcia Lucas*

### 3.1 INTRODUCTION

In order for a gamma ray to be detected, it must interact with matter; that interaction must be recorded. Fortunately, the electromagnetic nature of gamma-ray photons allows them to interact strongly with the charged electrons in the atoms of all matter. The key process by which a gamma ray is detected is ionization, where it gives up part or all of its energy to an electron. The ionized electrons collide with other atoms and liberate many more electrons. The liberated charge is collected, either directly (as with a proportional counter or a solid-state semiconductor detector) or indirectly (as with a scintillation detector), in order to register the presence of the gamma ray and measure its energy. The final result is an electrical pulse whose voltage is proportional to the energy deposited in the detecting medium.

In this chapter, we will present some general information on types of gamma-ray detectors that are used in nondestructive assay (NDA) of nuclear materials. The electronic instrumentation associated with gamma-ray detection is discussed in Chapter 4. More in-depth treatments of the design and operation of gamma-ray detectors can be found in Refs. 1 and 2.

### 3.2 TYPES OF DETECTORS

Many different detectors have been used to register the gamma ray and its energy. In NDA, it is usually necessary to measure not only the amount of radiation emanating from a sample but also its energy spectrum. Thus, the detectors of most use in NDA applications are those whose signal outputs are proportional to the energy deposited by the gamma ray in the sensitive volume of the detector.

#### 3.2.1 Gas-Filled Detectors

Gas counters consist of a sensitive volume of gas between two electrodes. (See Figure 3.1.) In most designs the outer electrode is the cylindrical wall of the gas pressure vessel, and the inner (positive) electrode is a thin wire positioned at the center of the cylinder. In some designs (especially of ionization chambers) both electrodes can be positioned in the gas separate from the gas pressure vessel.

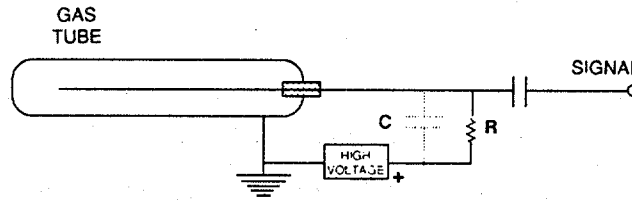


**Fig. 3.1** The equivalent circuit for a gas-filled detector. The gas constitutes the sensitive (detecting) volume. The potential difference between the tube housing and the center wire produces a strong electric field in the gas volume. The electrons from ionizations in the gas travel to the center wire under the influence of the electric field, producing a charge surge on the wire for each detection event.

An *ionization chamber* is a gas-filled counter for which the voltage between the electrodes is low enough that only the primary ionization charge is collected. The electrical output signal is proportional to the energy deposited in the gas volume.

If the voltage between the electrodes is increased, the ionized electrons attain enough kinetic energy to cause further ionizations. One then has a *proportional counter* that can be tailored for specific applications by varying the gas pressure and/or the operating voltage. The output signal is still proportional to the energy deposited in the gas by the incident gamma-ray photon, and the energy resolution is intermediate between NaI scintillation counters and germanium (Ge) solid-state detectors. Proportional counters have been used for spectroscopy of gamma rays and x rays whose energies are low enough (a few tens of keV) to interact with reasonable efficiency in the counter gas.

If the operating voltage is increased further, charge multiplication in the gas volume increases (avalanches) until the space charge produced by the residual ions inhibits further ionization. As a result, the amount of ionization saturates and becomes independent of the initial energy deposited in the gas. This type of detector is known as the *Geiger-Mueller (GM) detector*. A GM tube gas counter does not differentiate among the kinds of particles it detects or their energies; it counts only the number of particles entering the detector. This type of detector is the heart of the conventional  $\beta$ - $\gamma$  dosimeter used in health physics.

Gas counters do not have much use in gamma-ray NDA of nuclear materials. The scintillation and solid-state detectors are much more desirable for obtaining the spectroscopic detail needed in the energy range typical of uranium and plutonium radiation (approximately 100-1000 keV). Gas counters are described in more detail in Chapter 13, since they are more widely used for neutron detection.

### 3.2.2 Scintillation Detectors

The sensitive volume of a scintillation detector is a luminescent material (a solid, liquid, or gas) that is viewed by a device that detects the gamma-ray-induced light emissions [usually a photomultiplier tube (PMT)]. The scintillation material may be organic or inorganic; the latter is more common. Examples of organic scintillators are anthracene, plastics, and liquids. The latter two are less efficient than anthracene (the standard against which other scintillators are compared). Some common inorganic scintillation materials are sodium iodide (NaI), cesium iodide (CsI), zinc sulfide (ZnS), and lithium iodide (LiI). The most common scintillation detectors are solid, and the most popular are the inorganic crystals NaI and CsI. A new scintillation material, bismuth germanate ( $\text{Bi}_4\text{Ge}_3\text{O}_{12}$ ), commonly referred to as BGO, has become popular in applications where its high gamma counting efficiency and/or its lower neutron sensitivity outweigh considerations of energy resolution (Refs. 3 and 4). A comprehensive discussion of scintillation detectors may be found in Refs. 1, 2, and 5.

When gamma rays interact in scintillator material, ionized (excited) atoms in the scintillator material "relax" to a lower-energy state and emit photons of light. In a pure inorganic scintillator crystal, the return of the atom to lower-energy states with the emission of a photon is an inefficient process. Furthermore, the emitted photons are usually too high in energy to lie in the range of wavelengths to which the PMT is sensitive. Small amounts of impurities (called activators) are added to all scintillators to enhance the emission of visible photons. Crystal de-excitations channeled through these impurities give rise to photons that can activate the PMT. One important consequence of luminescence through activator impurities is that the bulk scintillator crystal is transparent to the scintillation light. A common example of scintillator activation encountered in gamma-ray measurements is thallium-doped sodium iodide [NaI(Tl)].

The scintillation light is emitted isotropically; so the scintillator is typically surrounded with reflective material (such as MgO) to minimize the loss of light and then is optically coupled to the photocathode of a PMT. (See Figure 3.2.) Scintillation photons incident on the photocathode liberate electrons through the photoelectric effect, and these photoelectrons are then accelerated by a strong electric field in the PMT. As these photoelectrons are accelerated, they collide with electrodes in the tube (known as dynodes) releasing additional electrons. This increased electron flux is then further accelerated to collide with succeeding electrodes, causing a large multiplication (by a factor of  $10^4$  or more) of the electron flux from its initial value at the photocathode surface. Finally, the amplified charge burst arrives at the output electrode (the anode) of the tube. The magnitude of this charge surge is proportional to the initial amount of charge liberated at the photocathode of the PMT; the constant of proportionality is the gain of the PMT. Furthermore, by virtue of the physics of the photoelectric effect, the initial number of photoelectrons liberated at the photocathode is proportional to the amount of light incident on the phototube, which, in turn, is proportional to the amount of energy deposited in the scintillator by the gamma ray (assuming no light

---

loss from the scintillator volume). Thus, an output signal is produced that is proportional to the energy deposited by the gamma ray in the scintillation medium. As discussed above, however, the spectrum of deposited energies (even for a monoenergetic photon flux) is quite varied, because of the occurrence of the photoelectric effect, Compton effect, and various scattering phenomena in the scintillation medium and statistical fluctuations associated with all of these processes. This is discussed in more detail in Section 3.3.

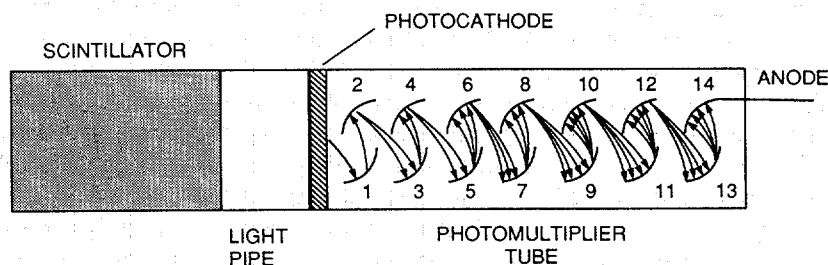


**Fig. 3.2** Typical arrangement of components in a scintillation detector. The scintillator and photomultiplier tube are often optically linked by a light pipe. The dynodes (1-13 in the figure) are arranged to allow successive electron cascades through the tube volume. The final charge burst is collected by the anode and is usually passed to a preamplifier for conversion to a voltage pulse.

### 3.2.3 Solid-State Detectors

In solid-state detectors, the charge produced by the photon interactions is collected directly. The gamma-ray energy resolution of these detectors is dramatically better than that of scintillation detectors; so greater spectral detail can be measured and used for SNM evaluations. A generic representation of the solid-state detector is shown in Figure 3.3. The sensitive volume is an electronically conditioned region (known as the *depleted region*) in a semiconductor material in which liberated electrons and holes move freely. Germanium possesses the most ideal electronic characteristics in this regard and is the most widely used semiconductor material in solid-state detectors. As Figure 3.3 suggests, the detector functions as a solid-state proportional counter, with the ionization charge swept directly to the electrodes by the high electric field in the semiconductor, produced by the bias voltage. The collected charge is converted to a voltage pulse by a preamplifier. The most popular early designs used lithium-drifted germanium [Ge(Li)] as the detection medium. The lithium served to inhibit trapping of charge at impurity sites in the crystal lattice during the charge collection process. In recent years, manufacturers have produced hyperpure germanium (HPGe) crystals, essentially eliminating the need for the lithium doping and simplifying operation of the detector.

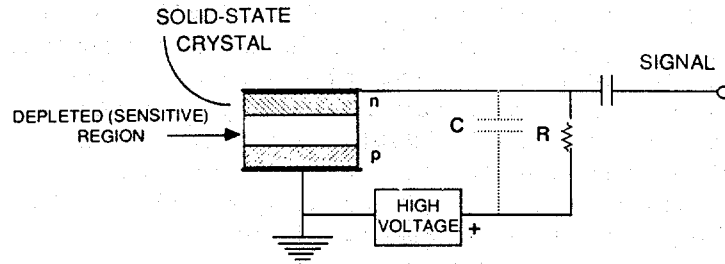


**Fig. 3.3** Typical arrangement of components in a solid-state detector. The crystal is a reverse-biased p-n junction that conducts charge when ionization is produced in the sensitive region. The signal is usually fed to a charge-sensitive preamplifier for conversion to a voltage pulse (see Chapter 4).

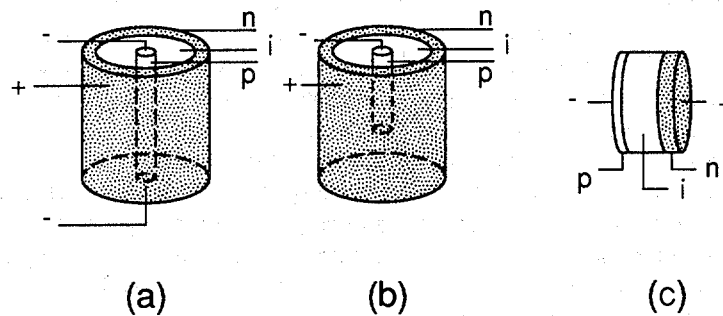


**Fig. 3.4** Illustration of various solid-state detector crystal configurations: (a) open-ended cylindrical or true coaxial, (b) closed-ended cylindrical, and (c) planar. The p-type and n-type semiconductor materials are labeled accordingly. The regions labeled i are the depleted regions that serve as the detector sensitive volumes. In the context of semiconductor diode junctions, this region is referred to as the intrinsic region or a p-i-n junction.

Solid-state detectors are produced mainly in two configurations: planar and coaxial. These terms refer to the detector crystal shape and the manner in which it is wired into the detector circuit. The most commonly encountered detector configurations are illustrated in Figure 3.4. *Coaxial detectors* are produced either with open-ended (the so-called true coaxial) or closed-ended crystals [Figure 3.4 (a-b)]. In both cases

the electric field for charge collection is primarily radial, with some axial component present in the closed-ended configuration. Coaxial detectors can be produced with large sensitive volumes and therefore with large detection efficiencies at high gamma-ray energies. In addition, the radial electric field geometry makes the coaxial (especially the open-ended coaxial) solid-state detectors best for fast timing applications. The *planar detector* consists of a crystal of either rectangular or circular cross section and a sensitive thickness of 1-20 mm [for example, Figure 3.4 (c)]. The electric field is perpendicular to the cross-sectional area of the crystal. The crystal thickness is selected on the basis of the gamma-ray energy region relevant to the application of interest, with the small thicknesses optimum for low-energy measurements (for example in the L-x-ray region for special nuclear material). Planar detectors usually achieve the best energy resolution, because of their low capacitance; they are preferred for detailed spectroscopy, such as the analysis of the complex low-energy gamma-ray and x-ray spectra of uranium and plutonium.

Because of their high resolution, semiconductor detectors are relatively sensitive to performance degradation from radiation damage. The amount of damage produced in the detector crystal per unit of incident flux is greatest for neutron radiation. Thus, in environments where neutron levels are high (such as accelerators, reactors, or instruments with intense neutron sources), the most significant radiation damage effects will be observed. Furthermore, radiation damage effects can be of concern in NDA applications where large amounts of nuclear material are continuously measured with high-resolution gamma-ray spectroscopy equipment—for example, in measurements of plutonium isotopics in a high-throughput mode.

The primary effect of radiation damage is the creation of dislocation sites in the detector crystal. This increases the amount of charge trapping, reduces the amplitudes of some full-energy pulses, and produces low-energy tails in the spectrum photopeaks. In effect, the resolution is degraded, and spectral detail is lost. An example of this type of effect is shown in Figure 3.5 (Ref. 6). It has been generally observed that significant performance degradation begins with a neutron fluence of approximately  $10^9$  n/cm<sup>2</sup>, and detectors become unusable at a fluence of approximately  $10^{10}$  n/cm<sup>2</sup> (Ref. 7). However, the new n-type HPGe crystals are demonstrably less vulnerable to neutron damage. Procedures have been described in which the effects of the radiation damage can be reversed through warming (annealing) the detector crystal (Ref. 8).

Further details on the design and use of solid-state detectors for gamma-ray spectroscopy may be found in Refs. 1, 2, and 9.

In the quiescent state, the reverse-bias-diode configuration of a germanium solid-state detector results in very low currents in the detector (usually in the pico- to nanoampere range). This leakage current can be further reduced from its room-temperature value by cryogenic cooling of solid-state medium, typically to liquid nitrogen temperature (77 K). This cooling reduces the natural, thermally generated electrical noise in the crystal but constitutes the main disadvantage of such detectors: the detector package must include capacity for cooling, and this usually involves a dewar for containing the liquid coolant. In recent years, attempts have been made

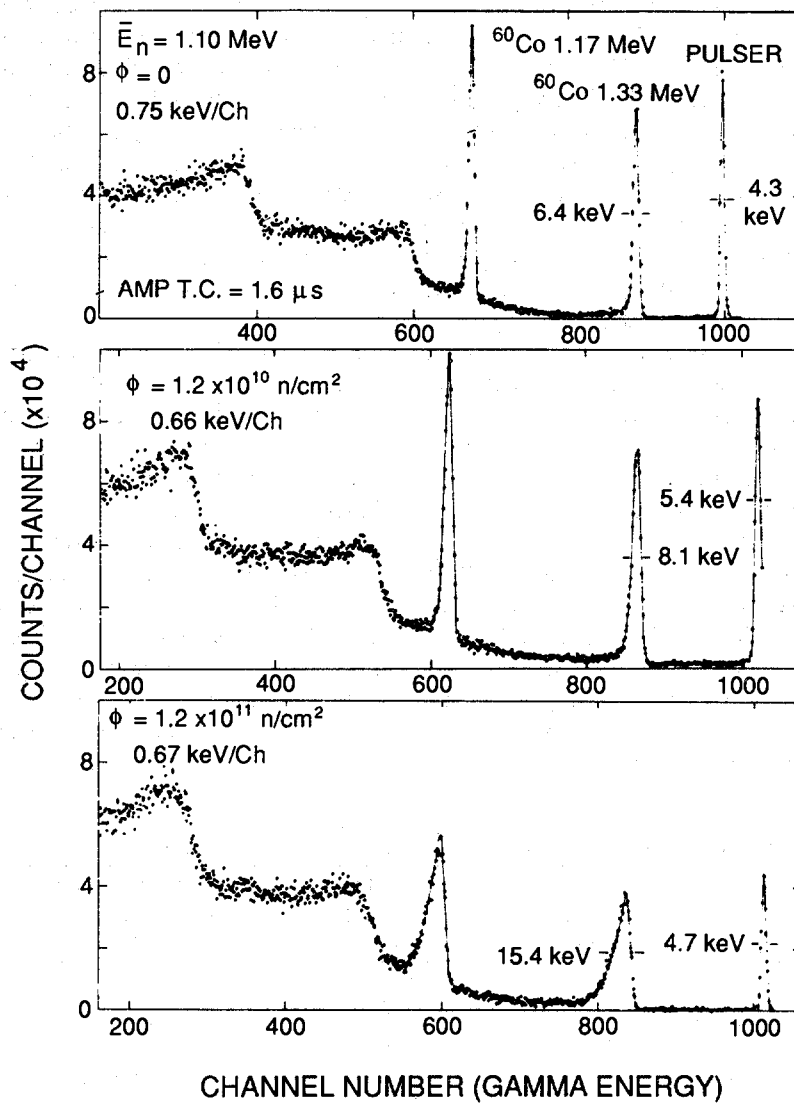


**Fig. 3.5** The deterioration of a high-resolution solid-state detector gamma spectrum with increasing neutron fluence ( $\phi$ ). The width of the 1.33-MeV  $^{60}\text{Co}$  photopeak is indicated in each spectrum. Only the high-energy portion of the spectrum is shown. Also noted is the width of an electronic pulser peak. (Adapted from Ref. 6.)

to cool the detector material electronically (Ref. 10), but these efforts are still in the experimental stages, and the capability is just beginning to be available commercially.

Another popular solid-state detector material for photon spectroscopy is lithium-drifted silicon [Si(Li)]. The lower atomic number of silicon compared to germanium reduces the photoelectric efficiency by a factor of about 50 (see Chapter 2), but this type of detector has been widely used in the measurement of x-ray spectra in the 1- to 50-keV energy range and finds some application in x-ray fluorescence (XRF) measurements (see Chapter 10). The low photoelectric efficiency of silicon above 50 keV is an advantage when measuring low-energy x rays and gamma rays, because it means that sensitivity to high-energy gamma rays is greatly reduced. Silicon detectors are most heavily used in charged-particle spectroscopy and are also used for Compton-recoil spectroscopy of high-energy gamma rays.

Other solid-state detection media besides germanium and silicon have been applied to gamma-ray spectroscopy. In NDA measurements, as well as many other applications of gamma-ray spectroscopy, it would be advantageous to have high-resolution detectors operating at room temperature, thereby eliminating the cumbersome apparatus necessary for cooling the detector crystal. Operation of room-temperature semiconductor materials such as CdTe, HgI<sub>2</sub>, and GaAs has been extensively researched (Ref. 11). Their higher average atomic numbers provide greater photoelectric efficiency per unit volume of material. Some of their performance characteristics are summarized in Table 3-1. However, these detector materials have enjoyed limited application to NDA problems to date, largely because it has not been possible to produce crystals sufficiently large for the total detection efficiencies needed in NDA applications. As crystal-growth technology improves, these detectors may become more attractive as convenient, high-resolution room-temperature detectors for gamma-ray spectroscopy of nuclear materials.

Table 3-1. Comparison of several semiconductor detector materials

Material	Atomic Numbers	Energy per e-h Pair ( $\delta$ ) <sup>a</sup> (eV)	Best $\gamma$ -Ray Energy Resolution at 122 keV <sup>b</sup> (keV)
Ge (77 K)	32	2.96	0.46
CdTe (300 K)	48, 52	4.43	3.80
HgI <sub>2</sub> (300 K)	80, 53	6.50	3.50
GaAs (300 K)	31, 33	4.2	2.60
NaI (300 K) <sup>c</sup>	11, 53		14.2

<sup>a</sup>This quantity determines the number of charge carriers produced in an interaction. (See Section 3.3.3.)

<sup>b</sup>Representative resolution data, as tabulated in Ref. 12. Energy resolution is discussed further in Section 3.3.3 and in Chapter 5.

<sup>c</sup>While not a semiconductor material, NaI is included in the table for convenient comparison.

### 3.3 CHARACTERISTICS OF DETECTED SPECTRA

In gamma-ray spectroscopy applications, the detectors produce output pulses whose magnitudes are proportional to the energy deposited in the detecting medium by the incident photons. The measurement system includes some method of sorting all of the generated pulses and displaying their relative numbers. The basic tool for accomplishing this task is the multichannel analyzer (MCA), whose operation is discussed in Chapter 4. The end result of multichannel analysis is a histogram (spectrum) of the detected output pulses, sorted by magnitude. The pulse-height spectrum is a direct representation of the energy spectrum of the gamma-ray interactions in the detection medium and constitutes the spectroscopic information used in gamma-ray NDA.

#### 3.3.1 Generic Detector Response

Regardless of the type of detector used, the measured spectra have many features in common. Consider the spectrum of a monoenergetic gamma-ray source of energy  $E_0$ . The gamma-ray spectrum produced by the decaying nuclei is illustrated in Figure 3.6(a). The gamma-ray photons originate from nuclear transitions that involve specific energy changes. There is a very small fluctuation in these energy values because of two effects: (1) the quantum uncertainties in the energies of the transitions (the so-called Heisenberg Uncertainty), and (2) recoil effects as the gamma-ray photons are emitted. These uncertainties are finite, but negligible compared with the other energy-broadening effects discussed below and so are not shown on the figure. Thus, the "ideal" monoenergetic gamma-ray spectrum from free decaying nuclei is essentially a sharp line at the energy  $E_0$ .

Since detected gamma-ray photons do not usually come from free nuclei but are emitted in material media, some of them undergo scattering before they emerge from the radioactive sample. This scattering leaves the affected photons with slightly less energy than  $E_0$ , and the energy spectrum of photons emitted from a material sample is slightly broadened into energies below  $E_0$  as shown in Figure 3.6(b). The magnitude of this broadening is also quite small with respect to other effects discussed below and is exaggerated in Figure 3.6(b) to call attention to its existence. It should also be noted that some gamma rays, after leaving the sample, will be scattered by external materials before entering the detector, and this effect can show up in the final energy spectrum (see below).

When the gamma ray enters the detection medium, it transfers part or all of its energy to an atomic electron, freeing the electron from its atomic bond. This freed electron then usually transfers its kinetic energy, in a series of collisions, to other atomic electrons in the detector medium.

The amount of energy required to produce electron-ion pairs in the detecting medium determines the amount of charge that will be produced from a detection event involving a given amount of deposited energy (see Table 3-1). A photoelectric interaction transfers all of the incident photon's energy to a photoelectron; this electron subsequently causes multiple ionizations until its energy is depleted. The amount of

---

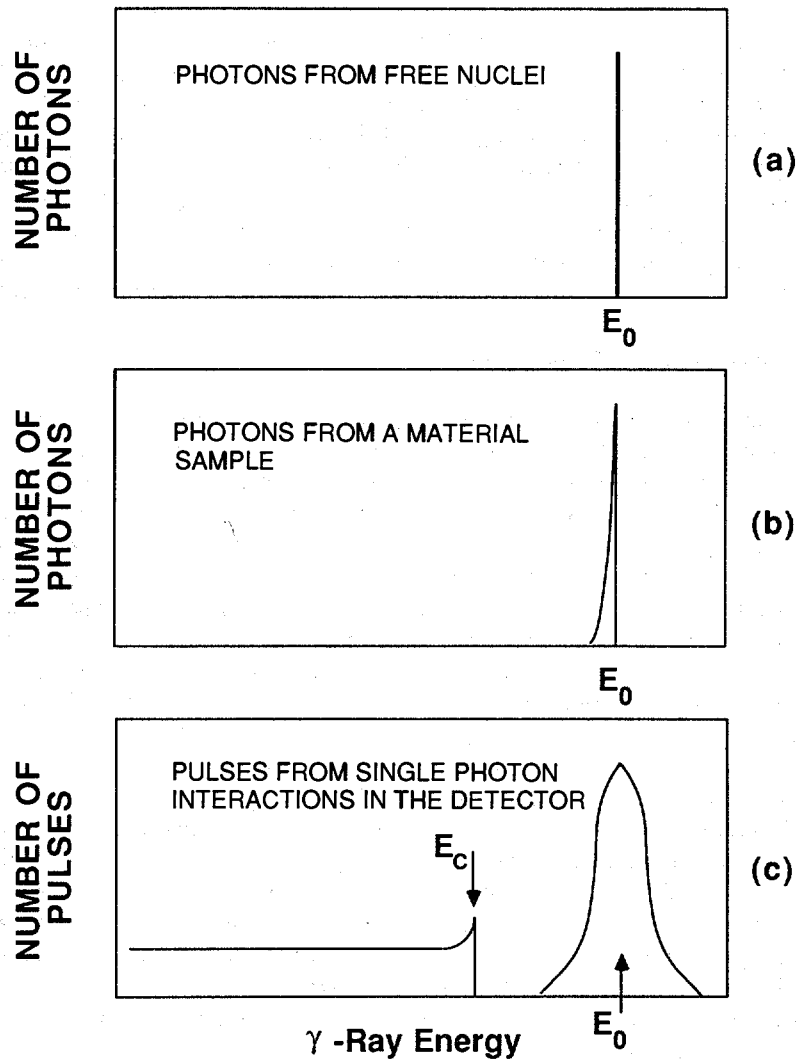


**Fig. 3.6** An idealization of the photon spectrum (a) produced by free nuclei, (b) emerging from a material sample, and (c) displayed from interactions in a detecting medium.

charge produced from this type of event is therefore proportional to the actual photon energy. A Compton scattering interaction transfers only part of the incident photon's energy to an ionized electron; and that electron subsequently causes ionizations until its energy is depleted. The amount of charge produced from this type of event is proportional to the partial energy originally lost by the incident photon but conveys no useful information about the actual photon energy. Multiple Compton scattering events for a single photon can produce amounts of charge closer to the value representing the full energy of the original photon; however, Compton-produced signals generally represent one scattering interaction and are lower in magnitude than the full-energy signals. The idealized detector response to the photoelectric and Compton interactions in the detection medium is shown in Figure 3.6(c). The maximum energy that can be deposited in the detection medium from a Compton scattering event comes from an event where the photon is scattered by  $180^\circ$ . The Compton-generated detector pulses are therefore distributed below this maximum energy [ $E_c$  in Figure 3.6(c)] and constitute a source of "background" pulses that carry no useful energy information.

The full-energy peak in Figure 3.6(c) is significantly broadened by the statistical fluctuation in the number of electron-ion pairs produced by the photoelectron. This effect is the primary contributor to the width of the full-energy peak and is therefore the dominant factor in the detector energy resolution (see Section 3.3.3).

### 3.3.2 Spectral Features

A more realistic representation of a detector-generated gamma-ray spectrum from a monoenergetic gamma-ray flux is shown in Figure 3.7. The spectral features labeled A-G are explained below.

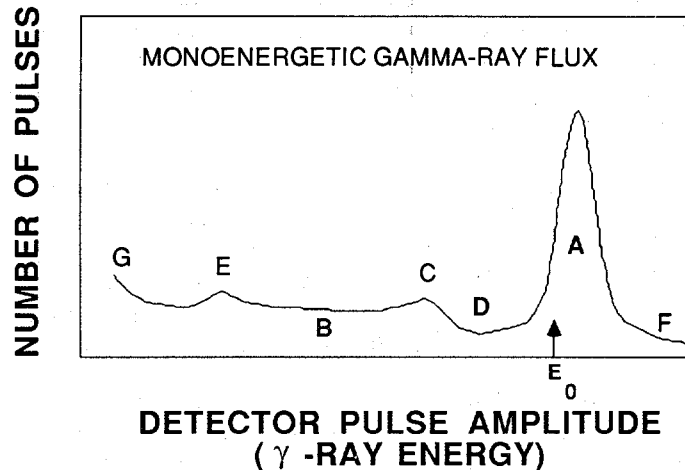


*Fig. 3.7 A realistic representation of the gamma detector spectrum from a monoenergetic gamma source. The labeled spectral features are explained in the text.*

**A. The Full-Energy Photopeak.** This peak represents the pulses that arise from the full-energy, photoelectric interactions in the detection medium. Some counts also arise from single or multiple Compton interactions that are followed by a photoelectric interaction. Its width is determined primarily by the statistical fluctuations in the charge produced from the interactions plus a contribution from the pulse-processing electronics (see Section 3.3.3 and Chapter 4). Its centroid represents the photon energy  $E_0$ . Its net area above background represents the total number of full-energy interactions in the detector and is usually proportional to the mass of the emitting isotope.

**B. Compton Background Continuum.** These pulses, distributed smoothly up to a maximum energy  $E_c$  (see Figure 3.6), come from interactions involving only partial photon energy loss in the detecting medium. Compton events are the primary source of background counts under the full-energy peaks in more complex spectra.

**C. The Compton Edge.** This is the region of the spectrum that represents the maximum energy loss by the incident photon through Compton scattering. It is a broad asymmetric peak corresponding to the maximum energy ( $E_c$ ) that a gamma-ray photon of energy  $E_0$  can transfer to a free electron in a *single* scattering event. This corresponds to a "head-on" collision between the photon and the electron, where the electron moves forward and the gamma-ray scatters backward through  $180^\circ$  (see Section 2.3.2). The energy of the Compton edge is given by Equation 2-11.

**D. The "Compton Valley."** For a monoenergetic source, pulses in this region arise from either multiple Compton scattering events or from full-energy interactions by photons that have undergone small-angle scattering (in either the source materials or intervening materials) before entering the detector. Unscattered photons from a monoenergetic source cannot produce pulses in this region from a *single* interaction in the detector. In more complex spectra, this region can contain Compton-generated pulses from higher-energy photons.

**E. Backscatter Peak.** This peak is caused by gamma rays that have interacted by Compton scattering in one of the materials surrounding the detector. Gamma rays scattered by more than  $110^\circ$ - $120^\circ$  will emerge with nearly identical energies in the 200- to 250-keV range. Therefore, a monoenergetic source will give rise to many scattered gamma rays whose energies are near this minimum value (see Ref. 1 and Section 2.3.2). The energy of the backscatter peak is given by Equation 2-10.

**F. Excess-Energy Region.** With a monoenergetic source, events in this region are from high-energy gamma rays and cosmic-ray muons in the natural background and from pulse-pileup events if the count rate is high enough (see Chapter 4). In a more complex spectrum, counts above a given photopeak are primarily Compton events from the higher-energy gamma rays.

**G. Low-Energy Rise.** This feature of the spectrum, very near the “zero-pulse-height-amplitude” region, arises typically from low-amplitude electronic noise in the detection system that is processed like low-amplitude detector pulses are. This noise tends to be at rather high frequency and so appears as a high-count-rate phenomenon. Electronic noise is usually filtered out of the analysis electronically (see Chapter 4), so this effect does not usually dominate the displayed spectrum. In more complex gamma-ray spectra, containing many different photon energies, the Compton-edge and backscatter peak features tend to “wash out,” leaving primarily full-energy peaks on a relatively smooth Compton background.

### 3.3.3 Detector Resolution

The resolution of a detector is a measure of its ability to resolve two peaks that are close together in energy. The parameter used to specify the detector resolution is the Full Width of the (full-energy) photopeak at Half its Maximum height (FWHM). If a standard Gaussian shape is assumed for the photopeak, the FWHM is given by

$$\text{FWHM} = 2\sigma\sqrt{\ln 2} \quad (3-1)$$

where  $\sigma$  is the width parameter for the Gaussian. High resolution (small FWHM) not only makes individual definition of close-lying peaks easier but also makes the subtraction of the Compton continuum less uncertain because it is a smaller fraction of the total activity in the peak region. The more complex a gamma-ray spectrum is, the more desirable it is to have the best energy resolution possible.

There are both natural and technological limits to how precisely the energy of a gamma-ray detection event can be registered by the detection system. The natural limit on the energy precision arises primarily from the statistical fluctuations associated with the charge production processes in the detector medium. The voltage integrity of the full-energy pulses can also be disturbed by electronic effects, such as noise, pulse pileup, improper pole-zero settings, etc. These electronic effects have become less important as technology has improved, but their potential effects on the resolution must be considered in the setup of a counting system. The electronic and environmental effects on detector resolution are discussed in more detail in Chapter 4.

The two types of detectors most widely used in gamma-ray NDA applications are the NaI(Tl) scintillation detector and the germanium solid-state detector. The NaI detector generates full-energy peaks that are much wider than their counterparts from the germanium detector. This is illustrated in Figure 3.8, where the wealth of detail evident in the germanium spectrum of plutonium gamma rays is all but lost in the corresponding NaI spectrum.

By considering the statistical limit on the energy precision, it is possible to understand the origin of the difference in the energy resolution achievable with various

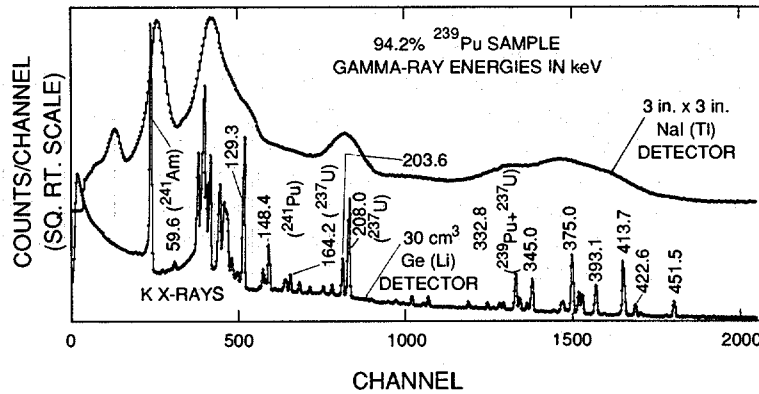


Fig. 3.8 Gamma-ray spectrum from a plutonium sample with 94.2%  $^{239}\text{Pu}$ , taken with a high-resolution solid-state detector [Ge(Li)] and with a NaI scintillation counter. Gamma-ray energies are given in keV.

types of detectors. Ideally, the number of electron charges ( $n$ ) produced by the primary detection event depends upon the total energy deposited ( $E$ ) and the average amount of energy required to produce an electron-ion pair ( $\delta$ ):

$$n = E/\delta . \quad (3-2)$$

The random statistical variance in  $n$  is the primary source of fluctuation in the full-energy pulse amplitude. However, for some detector types, this statistical variance is observed to be less than (that is, better than) the theoretical value by a factor known as the Fano factor (Ref. 13):

$$\sigma^2(n) = Fn = FE/\delta . \quad (3-3)$$

This effect comes from the fact that part of the energy lost by the incident photon goes into the formation of ion pairs and part goes into heating the lattice crystal structure (thermal energy). The division of energy between heating and ionization is essentially statistical. Without the competing process of heating, all of the incident energy would result in ion-pair production, and there would be no statistical fluctuation in  $n$  ( $F = 0$ ). By contrast, if the probability of ion pair production is small, then the statistical fluctuations would dominate ( $F \cong 1$ ). For scintillators, the factor  $F$  is approximately unity; for germanium, silicon, and gases, it is approximately 0.15 (Refs. 1 and 2). Since the number of charge carriers ( $n$ ) is proportional to the deposited photon energy (Equation 3-2), the *statistical portion* of the relative energy resolution is given by

$$\Delta E_{stat}/E = 2.35\sigma(n)/n = 2.35[F\delta/E]^{1/2} . \quad (3-4)$$

The statistical limits on detector resolution are compared in Table 3-2 for several types of detectors. The electronic contribution to the energy fluctuations ( $\Delta E_{elect}$ ) is essentially independent of photon energy and determined largely by the detector capacitance and the preamplifier. Thus, the total energy resolution can be expressed as the combination of the electronic and statistical effects:

$$\Delta^2 E_{tot} = \Delta^2 E_{elect} + \Delta^2 E_{stat} = \alpha + \beta E . \quad (3-5)$$

In Figure 3.9 (Ref. 14) the energy resolutions of scintillation, gas, and solid-state detectors are compared in the low-energy x-ray region. Techniques for measuring resolution are described in Section 5.2.

The argument presented here assumes that the scintillation efficiency is the main factor influencing the number of electrons produced at the photocathode of a scintillation detector. Other factors, such as scintillator transparency, play important roles. To work effectively as a detector, a scintillating material must have a high transparency to its own scintillation light. In a similar vein, factors such as charge carrier mobility

Table 3-2. Theoretical statistical energy resolution at 300 keV for different types of gamma-ray detectors

Detecting Medium	$\delta$ (eV) <sup>a</sup>	No. of Electrons, n, for 300 keV <sup>b</sup>	Relative Error in n <sup>c</sup>	Energy Resolution <sup>d</sup> (keV)	High-Energy Resolution <sup>e</sup> (keV)
Ge	2.96	$1.0 \times 10^5$	0.0032	0.86	1.60
Gas	30.	$1.0 \times 10^4$	0.010	2.73	--
NaI	-- <sup>f</sup>	$1.0 \times 10^3$	0.032	22.6	30.0
BGO	-- <sup>f</sup>	$8.0 \times 10^1$	0.11	77.6	100.0

<sup>a</sup>Average energy (in eV) required to produce one electron-ion pair in the detecting medium.

<sup>b</sup>The ratio  $E/\delta$  for  $E = 300$  keV (Equation 3-2).

<sup>c</sup>The quantity  $\sigma(n)/n$ , or  $(1/n)^{1/2}$ , without the incorporation of the Fano factor.

<sup>d</sup>The statistical portion of the energy resolution,  $\Delta E_{stat}$ , from Equation 3-4. Fano factors used were 0.15 for germanium and gas, and 1.0 for the scintillators. These are average values for purposes of illustration.

<sup>e</sup>Resolution at 1332 keV ( $^{60}\text{Co}$ ), calculated the same way as in the previous column, but using the higher energy. Values for gas detectors are not shown, since these detectors are ineffective for spectroscopy at such high energies.

<sup>f</sup>Since the measured charge is collected indirectly in scintillation detectors, this quantity is not relevant; a typical number of electrons produced at a photomultiplier photocathode per keV for NaI is taken from Ref. 1, and the numbers for BGO are based on the fact that its scintillation efficiency is approximately 8% of that for NaI (Ref. 1).

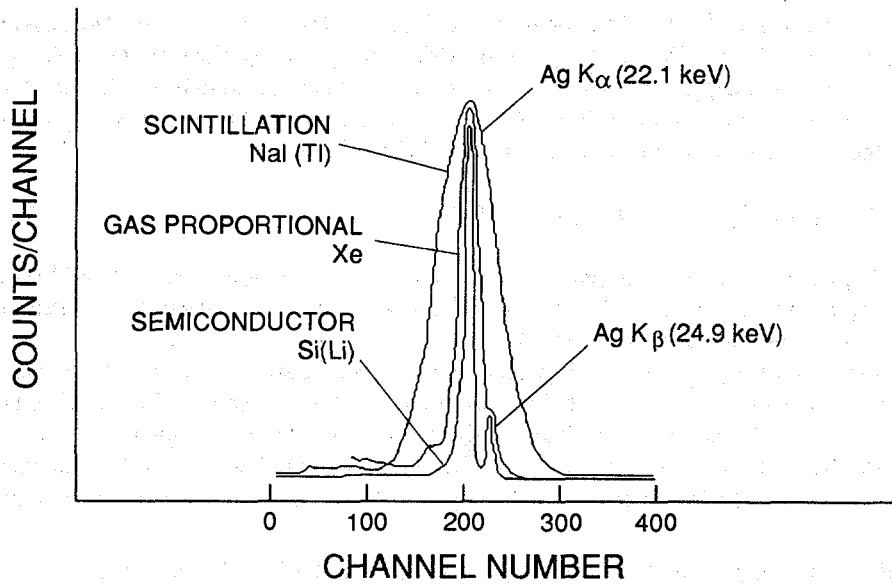


Fig. 3.9 Resolution comparison among NaI scintillation, gas proportional, and Si(Li) semiconductor detectors for the primary x rays of silver. (Adapted from Ref. 14.)

play an important role in determining the resolution of a solid state detector. This discussion is simplified of necessity, but it illustrates the primary reason why germanium detectors resolve so much better than scintillation detectors. See Ref. 1 for a more complete discussion of detector resolution.

### 3.3.4 Detector Efficiency

The basic definition of absolute photon detection efficiency is

$$\epsilon_{tot} = \frac{\text{total number of detected photons in the full-energy peak}}{\text{total number of photons emitted by the source}} \quad (3-6)$$

For the discussion to follow, we will be concerned with only full-energy events and thus with the full-energy detection efficiency. This total efficiency can be expressed as the product of four factors:

$$\epsilon_{tot} = \epsilon_{geom} \epsilon_{abs} \epsilon_{sample} \epsilon_{int} \quad (3-7)$$

The *geometric efficiency*  $\epsilon_{geom}$  is the fraction of emitted photons that are intercepted by the detector. For a point source this is given by

$$\epsilon_{geom} = A/(4\pi r^2) \quad (3-8)$$

where  $A$  is the cross-sectional area of the detector and  $r$  is the source-to-detector distance (described in Section 5.5). This factor is essentially independent of photon energy. It manifests the well-known inverse-square law for counting rates as a function of source-to-detector distance.

The *absorption efficiency*  $\varepsilon_{absp}$  takes into account the effects of intervening materials (such as the detector housing, special absorbers, etc.) that absorb some of the incoming radiation before it interacts with the detector volume. This term is especially important (it should be  $\ll 1$ ) for low-energy photons for which absorption effects are most pronounced. It has the mathematical form

$$\varepsilon_{absp} = \exp\left[-\sum \mu_i(E_\gamma)\rho_i x_i\right] \quad (3-9)$$

where  $\mu_i$ ,  $\rho_i$ , and  $x_i$  are the mass absorption coefficient, density, and thickness of the  $i$ th intervening material, and the summation is over all types of intervening materials.

The *sample efficiency*  $\varepsilon_{sample}$  is the reciprocal of the sample self-absorption correction ( $CF_{atten}$ ) discussed in Chapter 6. This quantity is the fraction of emitted gamma rays that actually emerge from the sample material. For example, in a slab of thickness  $x$  and transmission  $T$  equal to  $\exp[-(\mu\rho x)_s]$ , the sample efficiency is

$$\varepsilon_{sample} = \frac{1 - \exp[-(\mu\rho x)_s]}{(\mu\rho x)_s} = \frac{T - 1}{\ln T} \quad (3-10)$$

This factor clearly depends on the composition of each sample.

The *intrinsic efficiency*  $\varepsilon_{int}$  is the probability that a gamma ray that enters the detector will interact and give a pulse in the full-energy peak. In simplest terms, this efficiency comes from the standard absorption formula

$$\varepsilon_{int} = 1 - \exp(-\mu\rho x) \quad (3-11)$$

where  $\mu$  is the photoelectric mass attenuation coefficient, and  $\rho$  and  $x$  are the density and thickness of the sensitive detector material. This simple expression underestimates the true intrinsic efficiency because the full-energy peak can also contain events from multiple Compton scattering interactions. In general,  $\varepsilon_{int}$  is also a weak function of  $r$  because of the detection of off-axis incident gamma rays. Empirically,  $\varepsilon_{int}$  can usually be approximated by a power law of the form

$$\varepsilon_{int} \propto aE_\gamma^{-b} \quad (3-12)$$

Another important term is *relative efficiency*, which has two connotations:

- *Relative to NaI*: It is common practice to specify the efficiency of a germanium detector at 1332 keV ( $^{60}\text{Co}$ ) as a percent of the efficiency of a 3 in. by 3 in. NaI detector at 25-cm source-to-detector distance and the same gamma-ray energy:

$$\varepsilon_{rel\ to\ NaI}(\text{Ge}) = 100 \varepsilon_{tot}(\text{Ge}, 1332\ \text{keV}) / \varepsilon_{tot}(\text{NaI}, 1332\ \text{keV}) \quad (3-13)$$

The theoretical value of  $\epsilon_{tot}$  (NaI, 1332 keV) at 25 cm is  $1.2 \times 10^{-3}$ . Thus, for example, a 30% (relative) germanium detector has a theoretical absolute efficiency at 1332 keV at 25 cm of  $3.6 \times 10^{-4}$ .

- *Relative Efficiency Curve:* (Also called the intrinsic efficiency calibration.) This is a composite curve of the energy dependence of the ratio of the detected count rate to the emitted count rate:

$$\epsilon_{rel} = N\epsilon_{abs}\epsilon_{sample}\epsilon_{int} \quad (3-14)$$

The factor N emphasizes that, for most assay applications, the absolute value of this total efficiency is not as important as the relative values at different energies. This efficiency also includes the energy-dependent effect of the sample self-absorption  $\epsilon_{sample}$  (see Chapter 6 and Equation 3-10), and so must be determined for each sample measured.

The total relative efficiency may be calculated semi-theoretically, or (as is more prudent) it can be measured using many different gamma rays from one isotope. Aspects of this relative efficiency and its measurement are dealt with in greater detail in Chapter 8, and an example of a measured relative efficiency curve, including the sample self-absorption, is shown in Figure 8.14.

Detector efficiencies are usually measured and quoted as absolute photopeak efficiencies for detection of gamma rays from unattenuating point sources. Therefore, their energy dependence is dominated by  $\epsilon_{int}$  at the higher energies and by  $\epsilon_{abs}$  at the lower energies; the geometrical factor  $\epsilon_{geom}$  establishes the overall magnitude of the efficiency. The intrinsic and absorption efficiencies are strongly dependent on the incident photon energy, as illustrated in Figures 3.10 and 3.11 (Ref. 15), where the typical energy dependence of detector efficiency is shown for a planar and a coaxial Ge(Li) detector, respectively.

These figures make three general points:

1. The strong energy dependence of the total detection efficiency causes the recorded photon intensities to be significantly different from the emitted intensities. To perform quantitative assays involving comparison of the intensities of different gamma rays, one must take into account this energy-dependent efficiency correction.
2. When low-energy gamma-ray assays are performed, thin detector volumes should be used. This optimizes the detection efficiency in the low-energy region and reduces the detection efficiency for the unwanted high-energy gamma rays.
3. When high-energy gamma-ray assays are performed, thick detector volumes should be used to provide adequate efficiency for the more penetrating radiation. In addition, selected absorbers at the detector entrance can reduce contributions to the counting rate from unwanted low-energy radiation.

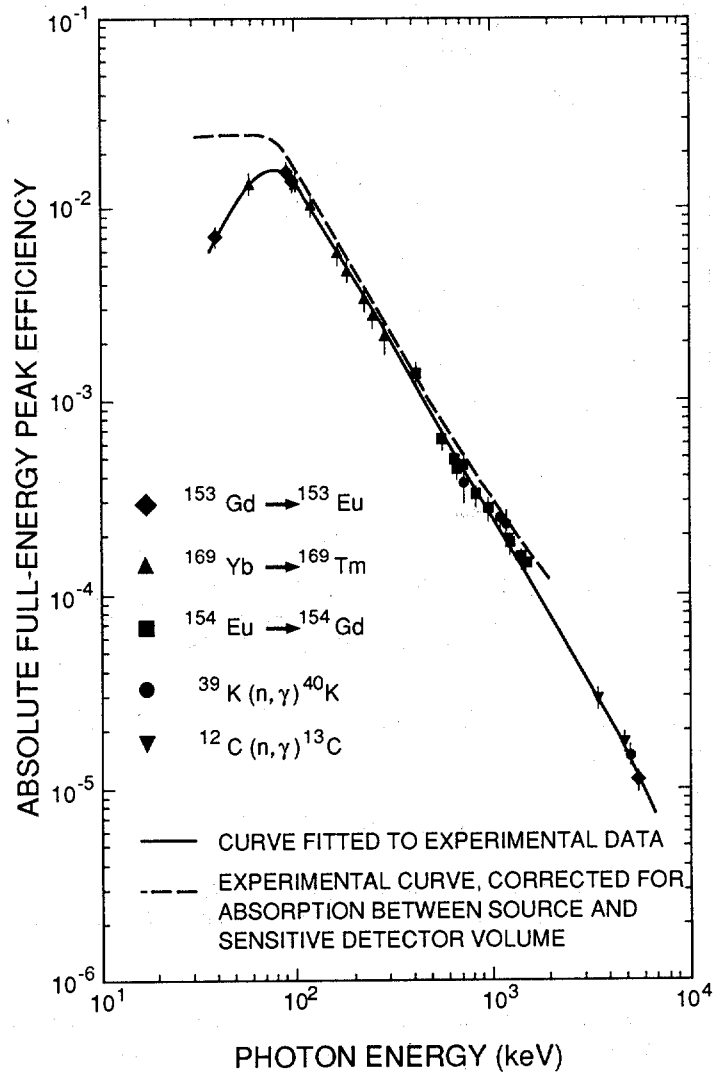


**Fig. 3.10** Absolute full-energy peak efficiency for a point source 54 mm from the face of a 33-mm-diam by 6.8-mm-thick planar Ge(Li) detector (adapted from Ref. 15). The measured data points are from known spontaneous and induced gamma decay processes. The low-energy decrease in efficiency illustrates the increased absorption of the low-energy incident radiation by the detector container and absorbers ( $\epsilon_{\text{abs}}$ ); the decrease in efficiency at high energy illustrates the decreased interaction rate in the detector crystal for higher-energy gamma rays ( $\epsilon_{\text{int}}$ ).

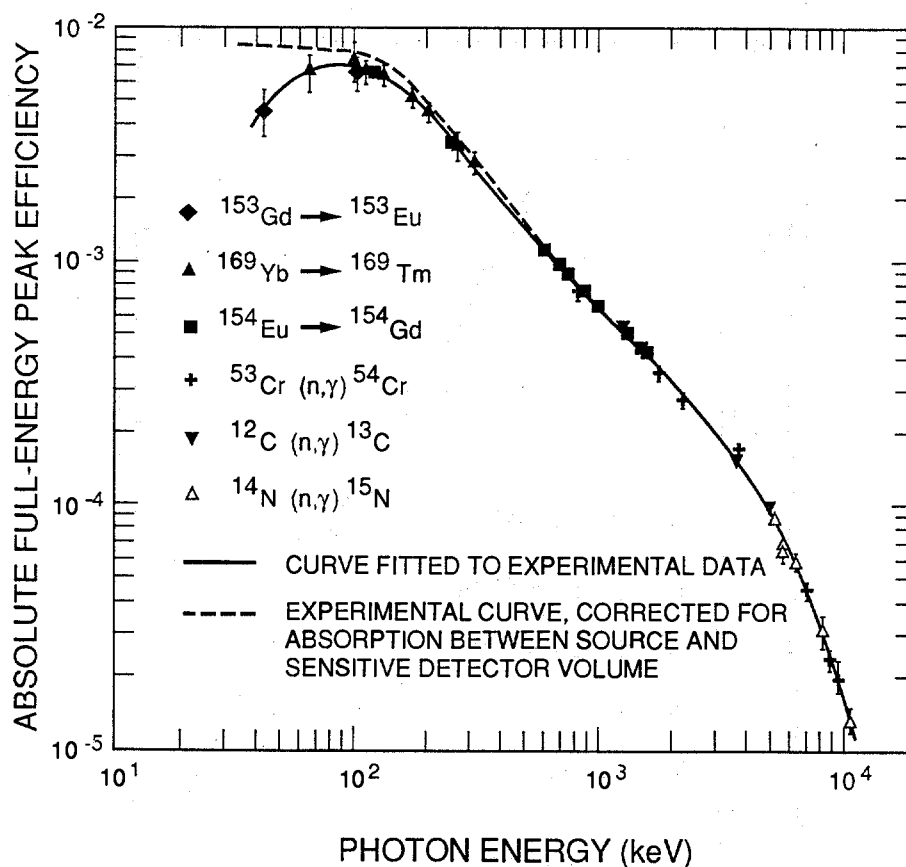


Fig. 3.11 Same as Figure 3.10, except for a point source 83 mm from the face of a 38-cm<sup>3</sup> true coaxial Ge(Li) detector (adapted from Ref. 15).

Even though Figures 3.10 and 3.11 illustrate these points for solid-state detectors, these same conclusions apply to NaI detectors as well. For example, uranium enrichment measurements at 186 keV are typically performed with a 2 in. by 1/2 in. scintillation crystal, while plutonium assays at 414 keV are usually done with axially thicker 2 in. by 2 in. scintillators.

### 3.4 DETECTOR SELECTION

Gamma-ray assay applications have varied objectives that can dictate the use of a variety of detectors. Discussion of the choice of detectors from the standpoint of energy resolution is given in Chapter 4. An additional consideration is the gamma-

ray (or x-ray) energy range of interest in a particular application. In general, the photon energies of major interest in the NDA of nuclear material range from below the x-ray region (85-100 keV) to approximately 400 keV. Exceptions are *L<sub>III</sub>*-edge densitometry in the 15- to 30-keV energy range (see Chapter 9), plutonium isotopic measurements in the 400- to 1000-keV range (see Chapter 8), and occasional measurements of <sup>238</sup>U daughter activity in the 600- to 1000-keV range. (The major gamma-ray signatures for nuclear material are listed in Table 1-2.) As was illustrated in the discussion above, detectors that are thick in the axial dimension are more efficient for the high-energy applications, and for low-energy gamma- and x-ray measurements, axially thin detectors are better suited because of their optimum detection efficiency at low to medium energies and relative insensitivity to higher-energy radiation. Other factors, such as cost and portability may dictate the use of less expensive and more portable NaI (scintillation) detectors, with the attendant sacrifice of good energy resolution. In recent years, high-resolution detectors have become available with small liquid-nitrogen dewars that render the detector assembly every bit as portable as a NaI detector. However, cost considerations still favor the scintillation detector over the high-resolution detector.

## REFERENCES

1. G. F. Knoll, *Radiation Detection and Measurement* (John Wiley & Sons, Inc., New York, 1979).
  2. F. Adams and R. Dams, *Applied Gamma-Ray Spectrometry* (Pergamon Press, New York, 1975).
  3. C. E. Moss, E. J. Dowdy, and M. C. Lucas, "Bismuth Germanate Scintillators: Applications in Nuclear Safeguards and Health Physics," *Nuclear Instruments and Methods A242*, 480 (1986).
  4. P. E. Koehler, S. A. Wender, and J. S. Kapustinsky, "Improvements in the Energy Resolution and High-Count-Rate Performance of Bismuth Germanate," *Nuclear Instruments and Methods A242*, 369 (1986).
  5. J. B. Birks, *The Theory and Practice of Scintillation Counting* (Pergamon Press, Oxford, 1964).
  6. H. W. Cramer, C. Chasman, and K. W. Jones, "Effects Produced by Fast Neutron Bombardment of Ge(Li) Gamma-Ray Detectors," *Nuclear Instruments and Methods 62*, 173 (1968).
-

7. P. H. Stelson, J. K. Dickens, S. Raman, and R. C. Trammell, "Deterioration of Large Ge(Li) Diodes Caused by Fast Neutrons," *Nuclear Instruments and Methods* 98, 481 (1972).
  8. R. Baader, W. Patzner, and H. Wohlfarth, "Regeneration of Neutron-Damaged Ge(Li) Detectors Inside the Cryostat," *Nuclear Instruments and Methods* 117, 609 (1974).
  9. R. H. Pehl, "Germanium Gamma-Ray Detectors," *Physics Today* 30, 50 (Nov., 1977).
  10. J. M. Marler and V. L. Gelezunas, "Operational Characteristics of High-Purity Germanium Photon Spectrometers Cooled by a Closed-Cycle Cryogenic Refrigerator," *IEEE Transactions on Nuclear Science* NS 20, 522 (1973).
  11. E. Sakai, "Present Status of Room-Temperature Semiconductor Detectors," *Nuclear Instruments and Methods* 196, 121 (1982).
  12. P. Siffert et al., "Cadmium Telluride Nuclear Radiation Detectors," *IEEE Transactions on Nuclear Science* NS 22, 211 (1975).
  13. U. Fano, "On the Theory of Ionization Yield of Radiation in Different Substances," *Physics Review* 70, 44 (1946); "Ionization Yield of Radiation II: The Fluctuations in the Number of Ions," *Physics Review* 72, 26 (1947).
  14. A. F. Muggleton, "Semiconductor X-Ray Spectrometers," *Nuclear Instruments and Methods* 101, 113 (1972).
  15. H. Seyfarth, A. M. Hassan, B. Hrastnik, P. Goettel, and W. Delang, "Efficiency Determination for some Standard Type Ge(Li) Detectors for Gamma Rays in the Energy Range from 0.04 to 11 MeV," *Nuclear Instruments and Methods* 105, 301 (1972).
-